Title

Structural and biochemical characterization of Leptospira interrogans Lsa45 reveals a penicillin-binding protein with esterase activity

Authors

Santos, Jademilson C

Handa, Sumit

Fernandes, Luis GV

et al.

Publication Date

2023-02-01

DOI

10.1016/j.procbio.2022.12.010

Peer reviewed

HHS Public Access

Author manuscript

Process Biochem. Author manuscript; available in PMC 2024 February 01.

Published in final edited form as:

Process Biochem. 2023 February ; 125: 141–153. doi:10.1016/j.procbio.2022.12.010.

Structural and biochemical characterization of *Leptospira interrogans* Lsa45 reveals a penicillin-binding protein with esterase activity

Jademilson C. Santos[a,e,*], **Sumit Handa**[b], **Luis G. V. Fernandes**[a], **Lucas Bleicher**[c], **César A. Gandin**[d], **Mario de Oliveira-Neto**[d], **Partho Ghosh**[b], **Ana Lucia T. O. Nascimento**[a,*]

[a]Laboratório de Desenvolvimento de Vacinas, Instituto Butantan, Avenida Vital Brasil, 1500, 05503-900, São Paulo, SP, Brazil.

[b]Department of Chemistry & Biochemistry, University of California, San Diego, CA 92093, USA.

[c]Departamento de Bioquímica e Imunologia, Instituto de Ciências Biológicas (ICB), Universidade Federal de Minas Gerais (UFMG), Belo Horizonte, Brazil.

[d]Universidade Estadual Paulista (UNESP), Instituto de Biociências, Dep. de Física e Biofísica, Botucatu, SP, Brazil

[e]Instituto Federal da Bahia – IFBA - Rodovia BR-367, R. José Fontana, 1, 45810-000, Porto Seguro - BA, Brazil.

Abstract

Leptospirosis is a bacterial disease that affects humans and animals and is caused by *Leptospira*. The recommended treatment for leptospirosis is antibiotic therapy, which should be given early in the course of the disease. Despite the use of these antibiotics, their role during the course of the disease is still not completely clear because of the lack of effective clinical trials, particularly for severe cases of the disease. Here, we present the characterization of *L. interrogans* Lsa45 protein by gel filtration, protein crystallography, SAXS, fluorescence and enzymatic assays. The oligomeric studies revealed that Lsa45 is monomeric in solution. The crystal structure of Lsa45 revealed the presence of two subdomains: a large α/β subdomain and a small α-helical subdomain. The large subdomain contains the amino acids Ser122, Lys125, and Tyr217, which correspond to the catalytic triad that is essential for β-lactamase or serine hydrolase activity in similar enzymes. Additionally, we also confirmed the bifunctional promiscuity of Lsa45, in

[*]To whom correspondence should be addressed: Ana L. T. O. Nascimento - ana.nascimento@butantan.gov.br - Laboratório de Desenvolvimento de Vacinas, Instituto Butantan, Avenida Vital Brasil, 1500, 05503-900, São Paulo, SP, Brazil, Jademilson C. Santos – jademilsonsantos@gmail.com – Instituto Federal da Bahia – IFBA - Rodovia BR-367, R. José Fontana, 1, 45810-000, Porto Seguro - BA, Brazil.

Author contributions

JCS and ALTO conceived the idea of the study. JCS, SH, LGVF, LB, CAG and MON performed the experiments. JCS, SH, LGVF, LB, CAG, MON, PG and ALTO analyzed the data and wrote the manuscript.

Conflict of Interest

The authors declare no conflict of interest.

hydrolyzing both the 4-nitrophenyl acetate (*p*-NPA) and nitrocefin β-lactam antibiotic. Therefore, this study provides novel insights into the structure and function of enzymes from *L. interrogans*, which furthers our understanding of this bacterium and the development of new therapies for the prevention and treatment of leptospirosis.

Graphical Abstract

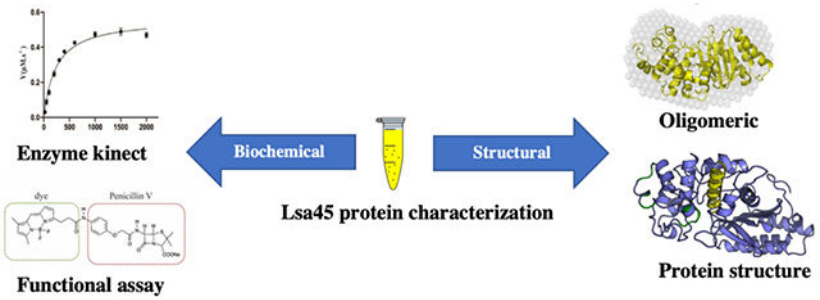

Keywords

L. interrogans ; bifunctional enzyme; β-lactamase/esterase; PBP; crystal structure; leptospirosis

1. Introduction

Leptospirosis is a widespread zoonotic disease caused by pathogenic spirochaetes of the genus *Leptospira*, a Gram-negative bacterium with a high prevalence in tropical and subtropical regions and with considerable impacts on public health [1]. The transmission of leptospirosis has been associated with exposure of individuals to wild or farm animals. Recently, the disease has become prevalent in cities with sanitation problems and large populations of urban rodents, which contaminate the environment through their urine [2,3].

Human leptospirosis has diverse clinical aspects and progression, with symptoms appearing around 10 days after infection. In milder disease presentations, the symptoms are fever, chills, vomiting, nausea, headache, cough, and diarrhea. The majority of leptospirosis infections are self-limiting, resulting in infection resolving without the necessity for antibiotics; however, about 10% evolve into a severe multisystemic manifestation termed Weil syndrome, with significant rates of morbidity and mortality when not properly treated [4,5].

Since most initial symptoms of leptospirosis resemble those of other tropical febrile diseases, such as malaria, rickettsial infection, influenza, dengue and bacterial sepsis [4,6], leptospirosis is often misdiagnosed or underdiagnosed. Furthermore, culturing bacteria from clinical samples is not a trivial task, due to the fastidious nature of pathogenic leptospires and their requirement for special media, such as EMJH [7] and, more recently, HAN [8]. The microscopic agglutination test (MAT) is currently the reference method for diagnosis of leptospirosis, consists of *in vitro* agglutination of a panel of live leptospires by antibodies in the serum samples of suspected patients. Added to the laborious and technical nature of this test, MAT sensitivity is extremely low at the onset of the disease [9].

All these difficulties in diagnosis can hinder the initial treatment, a point in time at which antibiotic therapy is more effective, leading to an increase in leptospirosis mortality [6,10]. Despite the Leptospira to be susceptible to a variety of antibiotics, it is not clear which should be choice to treatment. The antibiotics available in the literature includes penicillin, doxycycline, cefotaxime, ceftriaxone and azithromycin. Historically, members of the penicillin group were the first drugs used in the fight against leptospirosis [11]. In alternative cases, oral doxycycline could be used, but concerns exist regarding its use in all patients [12,13]. A meta-analysis of clinical trials of leptospirosis treatment with ten antibiotics compared with control placebo groups showed no difference between penicillin treatment and placebo with regard to mortality[14]. The efficacy of using penicillin to mitigate other consequences of leptospirosis, such as the need for dialysis and liver function damage, was not established. Moreover, no difference was observed in the therapy of leptospirosis when using penicillin, cephalosporins or doxycycline [15]. Third generation cephalosporins such as cefotaxime and ceftriaxone are commonly used in the treatment of leptospirosis. In many cases, these may be the preferred agents, mainly in severe leptospirosis with febrile illness when the diagnosis is in doubt with other etiologies[16]. Few studies using carbapenems against Leptospira have been performed. In one of these studies, an *in vivo* model of acute leptospirosis using ertapenem antibiotic was evaluated. Measurement of the survival rate and clearance of leptospira in the organs liver, kidney, lung, heart and spleen has been shown even in small doses of ertapenem [17]. However, similar to other antibiotics such as, fluoroquinolone, chloramphenicol and azithromycin which also were tested against leptospira, more human trials are necessary to fully support their use [12,16].

β-Lactams interact with both penicillin-binding proteins (PBPs) and β-lactamases, a large family of serine hydrolases that are involved in the biosynthesis and maintenance of bacterial peptidoglycan [18]. Despite their binding, the two groups have distinct functions. Whereas PBPs catalyze the final transpeptidation reaction of bacterial cell wall biosynthesis, β-lactamases, which account for the most common mechanism of bacterial resistance to β-lactam antibiotics, catalyze the opening of the β-lactam ring by efficiently hydrolyzing its amide group [19]. On the basis of their amino acid sequence, PBPs have been classified into two groups, high-molecular-weight (HMW) PBPs and low-molecular-weight (LMW) PBPs. In some bacteria, such as *Escherichia coli*, the HMW PBPs can be bifunctional (transglycosylase/transpeptidase) and are important targets of β-lactams. The LMW PBPs can be a monofunctional carboxypeptidase, endopeptidase, or bifunctional carboxypeptidase/endopeptidase.

Several leptospiral surface proteins have been explored regarding their potential in mediating host-pathogen interaction, via direct binding to host extracellular matrix and plasma components [20,21]. One such leptospiral receptor, namely Lsa45 (Leptospiral surface adhesin of 45 kDa) was predicted as outer-membrane lipoprotein and characterized as a laminin and plasminogen-binding protein, being correlated to bacterial colonization and invasion processes; furthermore, reactivity to confirmed leptospirosis serum samples corroborates the expression of its native counterpart during mammalian infection [22]. *In silico* analysis have shown that Lsa45 protein contains a β-lactamase domain, but this property and its implications remained to be explored.

Here, we present the crystal structure of Lsa45, a protein previously described[22], revealing a bifunctional enzyme that has two subdomains: a large α/β subdomain and a small α-helical subdomain. The structure allowed us to understand the functionality of Lsa45; the protein was characterized as a PBP with weak affinity for β-lactams. Additionally, Lsa45 exhibited an esterase functionality with activity against 4-nitrophenyl acetate (*p*-NPA) as substrate. These structural and biochemical findings may help shed light on the mechanism of action of antibiotics in the treatment of leptospirosis.

2. Materials and Methods

2.1 Protein expression and purification

The gene coding for Lsa45 (LIC10731) was cloned into pAE vector with an N-terminal 6xHis-Tag [22]. *E. coli* BL21 (DE3) containing plasmid pGro7 (Takara Bio Inc., Shiga, Japan) expressing *groES-groEL* was transformed with the plasmid pAE-Lsa45. After plating, a single colony was inoculated in 5 mL of lysogeny broth medium (LB-medium) containing 100 μg/mL ampicillin and 30 μg/mL chloramphenicol and grown at 37 °C for 16 h. The inoculum was transferred to 1 L of LB medium containing the two selection antibiotics and supplemented with 1 mg/mL L-arabinose to induce the expression of the chaperones. The culture was grown with shaking at 37 °C until OD600nm 0.6–1.0. The temperature was then lowered to 22 °C and protein expression induced with 1 mM IPTG. The bacterial culture was then grown further with shaking for 16 h.

Cells were harvested by centrifugation for 20 min at 6000 rpm and resuspended in 50 mL buffer A (20 mM Tris-HCl, pH 7.8, 200 mM NaCl, 10 % glycerol and 1 mM PMSF). The cells were disrupted with 500 μL lysozyme solution (10 mg/mL), incubated on ice for 15 min, and sonicated with 5 cycles of 30 s on/off. The cell debris was removed by centrifugation at 15,000 rpm for 45 min at 8 °C. The clarified solution was loaded on a Ni-NTA HisTrap HP column (GE Healthcare) pre-equilibrated with buffer B (20 mM Tris-HCl, pH 7.8, 150 mM NaCl and 5% glycerol). Lsa45 was eluted in buffer B containing 500 mM imidazole. The protein sample was concentrated to 2 mL and loaded onto a size-exclusion chromatography (SEC) HiLoad Superdex 200 16/600 column (GE Healthcare), which was pre-equilibrated with buffer B. The peak fractions corresponding to purified protein were verified by SDS-PAGE.

2.2 Crystallization and data collection

Initial screening was carried out using commercials kits in a HoneyBee 963 (Digilab Global) robot dispensing into a 96-well plate through the sitting-drop vapor diffusion technique. Crystals were obtained at 20 °C with 0.20 μL of the protein concentrate to 12 mg/mL and 0.20 μL of reservoir solution consisting of 100 mM Tris-HCl, pH 8.5, 30% PEG 1500 and 8% MPD. The optimization of conditions was performed in a 24-well plate using the hanging-drop vapor-diffusion method with a reservoir volume of 500 μL and a drop size of 2 μL (1:1 ratio of reservoir: protein).

For data collection, crystals were harvested with a nylon loop and soaked for up 2 min into a solution similar to the precipitant solution, but which was supplemented with 0.5 M KI.

After, the crystals were transferred to a cryoprotect solution containing the crystallization solution and 15 % ethylene glycol and then flash cooled to 100 K in N_2 [23,24]. Diffraction data were collected to 1.62 Å resolution limit on MX2 beamline at the LNLS (Campinas, SP, Brazil) using a 1.5499 Å wavelength X-ray beam and a PILATUS2M detector (Dectris, Baden-Dattwil, CHE). The data were processed using XDS [25] and scaled with AIMLESS using CCP4 [26].

2.3 Structure determination and refinement

The structure of Lsa45 was determined by the single-wavelength anomalous dispersion (SAD) method using iodide ions as anomalous scatterers [24]. The iodide site searches, phasing and density modification was carried out using AutoSol [27]. Initial model located 48 iodide ion sites and overall Figure of Merit (FOM) from 0.352. The initial model was built into density-modified electron density maps using AUTOBUILD [28]. The final model was refined using PHENIX [29] and model building was carried out with Coot [30]. The quality of the structure was evaluated with MOLPROBITY [31] and PDB-REDO web server [32]. Atomic coordinates and structure factors were deposited in the Protein Data Bank (PDB) with accession code 8DC1. Analyses of the structures were performed with PyMOL [33] and DALI server that use C-alpha aligned [34]. The substrate-binding pocket in Lsa45 was predicted using the POCASA server [35]. The data collection and refinement statistics are detailed in Table 1.

2.4 Oligomeric state solution

Molecular mass determination based on SEC retention volume was performed as follows. The sample was centrifuged at 4 °C for 5 min at 15,000 rpm to remove aggregates. Two mL of the protein solution at 5 mg/mL were applied to a HiLoad Superdex 200 16/60 column (GE Healthcare), pre-equilibrated with a buffer composed of 20 mM Tris-HCl, pH 7.8, 150 mM NaCl and 5 % glycerol and run in the same buffer. The standard curve for the column was based on ferritin (440 kDa), aldolase (158 kDa), conalbumin (75 kDa) carbonic anhydrase (29 kDa) and ribonuclease (13.7 kDa) from the Gel Filtration Calibration Kit (GE Healthcare). Protein elution volume was monitored by absorbance at 280 nm. All molecular weight values were assessed using a molecular weight standard curve.

Small-angle X-ray scattering (SAXS) data were collected for Lsa45 at 1 and 10 mg/mL at the D02A-SAXS1 beamline of the Brazilian Synchrotron Light Laboratory (LNLS/CNPEM – Campinas – Brazil). The monochromatic incident radiation was set at a wavelength of 1.54 Å. The sample-detector distance was 888 mm, resulting in a scattering vector q (defined as $q = 4\pi\sin\theta/\lambda$, where 2θ is the scattering angle) ranging from $0.013\ Å^{-1} < q < 0.497\ Å^{-1}$. For monitoring radiation damage in the samples during the SAXS measurements, five consecutive frames of sixty seconds were recorded in a two-dimensional Pilatus detector. SAXS intensities were corrected for the detector response, intensity of the incident beam, sample absorption and buffer scattering. The 2D scattering patterns were integrated using the Fit2D software [36] and the resulting one-dimensional scattering curve.

Fitting of the experimental data and adjustment of the pair-distance distribution function, *p(r)*, were conducted using Gnom software from the ATSAS Package. The low-resolution

model was generated using the "*ab initio*" routine implemented on the dammif/dammin software [37]. SAXS pattern simulation, based on the crystallographic structure, was determined using Crysol. Molecular weight was calculated using the SAXSMoW2 [38].

2.5 Bocillin FL binding assay

PBP function was tested with fluorescent penicillin Bocillin FL (Fisher Scientific - Hampton, NH). Bocillin FL is a fluorescent derivative of penicillin V that has been used to validate PBP and β β β β β β -lactamase binding studies [39]. Several reactions were carried out containing 5 μL of Lsa45 (5 mg/mL) in PBS buffer and Bocillin FL (0, 50, 100, 200, 300, 500 and 1000 μM) in a total volume of 50 μL. As a negative control, a fragment of Enterococcal surface protein (Esp, aa 48–452) was used [40]. All reactions were incubated for 2 h at 37 °C and stopped by addition of 20 μL SDS-PAGE loading buffer (125 mM Tris-HCl, 4% SDS, 20% glycerol, 2% 2-mercaptoethanol, pH 6.8). The reactions were boiled for 5 min. Twenty μL of each sample were loaded onto a 12% SDS-PAGE gel and resolved by electrophoresis. The gel was developed and scanned using a Molecular Imager® Gel Doc™ XR (BioRad). The fluorescent bands were quantified using Image Lab™ software.

2.6 Enzymatic activity and kinetic parameters

To reproduce the physiological conditions, the Lsa45 purification buffer was exchanged for the PBS buffer. The β-lactamase activity of Lsa45 was determined using nitrocefin (Cayman Chemical - Ann Arbor, MI), a chromogenic β-lactam substrate that in the presence of β-lactamase activity changes color [41]. The reaction was prepared using 0–250 μg Lsa45 protein and 100 μM nitrocefin in PBS buffer. The color development was measured by absorbance at 482 nm. The esterase activity of Lsa45 was determined with 4-nitrophenyl acetate (*p*-NPA; Fisher Scientific - Hampton, NH) by measuring the absorbance at 405 nm. The standard assay solution consisted of 100 μM *p*-NPA in PBS buffer with 0–50 μg Lsa45 protein. Both reactions were incubated for 1 h at 20, 28 or 37 °C.

Lsa45 activities were assayed by monitoring hydrolysis of nitrocefin and *p*-NPA in a Spark multimode reader (Tecan) at 37 °C. The reactions were conducted in triplicate and were started by adding the enzyme at a final concentration of 0.6 mg/mL for nitrocefin ($\Delta\varepsilon_{482}$= 17,400 $M^{-1}.cm^{-1}$) and 0.25 mg/mL for *p*-NPA ($\Delta\varepsilon_{405}$= 13,294 $M^{-1}.cm^{-1}$). The measurement was monitored for 180 s. Kinetic parameters, V_{max}, k_{cat} and K_m, were obtained by varying the concentration of nitrocefin (20–200000 μM) and *p*-NPA (10–2000 μM). Steady-state kinetic parameters were obtained by fitting reaction curves to the Michaelis–Menten equation using GraphPad Prism 8.

2.7 Sequence coevolution analysis

To detect functionally relevant positions in Lsa45, we performed a coevolution analysis using the decomposition of residue coevolution networks (DRCN) method [42] as implemented in the PFstats software [43]. DRCN detects sets of residues that tend to appear simultaneously (coevolve) in sub-sets of a protein family represented by a multiple sequence alignment. It has been observed that such sets usually report the determinants of sub-family specific characteristics such as enzymatic activity (coevolution of catalytic

residues), specificity (coevolution in residues ligand recognition pockets), disulfide bridges (coevolution between cysteine pairs), DNA binding (formation of P-boxes), etc. A multiple sequence alignment from the β-lactamase family was obtained from Pfam [44]. To remove fragments and redundancy, the alignment was filtered and sequences not having 90% of the positions in the HMM for this protein family were removed (Pfam accession code: PF00144), followed by a filter of 70% identity. The final alignment was used to detect groups of coevolving positions using a standard PFstats protocol: a pair of residues is considered to be correlated when both are present in at least 10% of the sequences, the presence of the first increases the frequency of the other to more than 80%, and the associated p-value to that frequency shift is less than 10^{-10}. Residues are considered to be anti-correlated if the same conditions apply but the shift is negative, with the presence of one residue causing a frequency decrease in the other to less than 20%. After the set of correlated pairs are identified, the definition of coevolving sets is obtained by a trivial clustering procedure: a residue is considered to belong to a coevolving set if it is correlated to at least one of the other members in the set.

3. Results and Discussion

3.1 Overall structure and structural analyses of Lsa45

The crystal structure of Lsa45 was determined in apo form by the SAD method to 1.62 Å resolution limit. The Matthews coefficient value suggested the presence of one molecule in the asymmetric unit corresponding to 42% solvent content [45]. The crystal belongs to the orthorhombic space group $P2_12_12_1$. The final model includes 214 waters, 1 PEG, 2 ethylene glycols and 15 iodide molecules. A final map shows a well-defined electron density throughout most of the structure, which includes amino acids 64–398. Some amino acids were not included in the final model because the electron density was missing. These amino acids are presumed to be disordered and correspond to loop regions present in the N-terminal (36–57) and C-terminal (399–419) subdomains, which also was observed in many other structures with similar fold [46–48]. The Lsa45 structure adopts a two-subdomain structure composed of a small α-helix subdomain and a large α/β subdomain, which is also present in other serine hydrolases, such as family VIII esterase [48], PBPs [19], AD-peptidase [49] and class C β-lactamases [50]. The large α/β subdomain consists of a six-stranded antiparallel β-sheet in the middle (β2, β1, β6, β5, β4 and β3) flanked by five helices on one side (α1, α2, α14, α11, α15 and α16) and four helices on the other side (α3, α11, α12 and α13). The small α-helix subdomain includes seven α-helices (α4, α5, α6, α7, α8, α9 and α10) (Fig. 1A). The N- and C-terminal regions that comprise the large subdomain has higher values of *B*-factor of Lsa45. Fig. 1B is colored according to the *B*-factor value of C α atoms. The high value *B*-factor are related to atom packing in proteins, but in many studies this value has been extensively used to investigate protein flexibility [51].

Structural alignment of Lsa45 with known structures of homologs deposited in PDB showed various structural similarities with other proteins from different organisms. The four most pronounced functions found in Dali were those of PBPs [49,52], class C β-lactamases [53–55], peptidases [49] and esterases [56–58], suggesting that Lsa45 has one of these

functions. The first structural characteristic compared to Lsa45 was the substrate-binding pocket. Like other members of the α/β hydrolase family, the substrate-binding pocket is positioned in a groove between the large α/β subdomain and small α-helix subdomain, at the edge of the central β-sheet of the α/β subdomain. The volume of the putative substrate-binding pocket was determined for Lsa45, which had a small volume of 127 $Å^3$ (Fig. 2), differing from some structural homolog proteins that have moderate to larger volumes for the substrate-binding pocket, such as *Escherichia coli* AmpC (*EcAmpC*) - 225.0 $Å^3$, *Caulobacter crescentus* EstA (*CcEstA*) - 267.8 $Å^3$ and *Pyrococcus abyssi* PBP (*PaPBP*) - 1963.7 $Å^3$ [46,50]. In addition to the size, the shape of the binding pocket also differs significantly between the proteins. The surface charge in the Lsa45 cleft is mostly positive due to the high content of arginine and lysine, which corresponds to 14.1% of structure. This environment facilitates binding to negatively charged substrates. The importance of binding pocket size and shape has been studied for the different α/β hydrolases, and it has been established that these characteristics may directly affect access, recognition and substrate specificity [49,59]. In Lsa45 and *Ec*AmpC, access to the binding pocket is free, thus leaving enough space for bulkier substrates to enter but with shapes completely different, where Lsa45 has a rectangular shape and *Ec*AmpC a diffuse shape. The substrate-binding pocket of *Pa*PBP is larger and diffuse with access to the substrate only restricted by a α-helix (residues 113–126). In the case of *Cc*EstA, the α5/α6 and β3/β4 loops limit substrate access to the substrate-binding pocket. The substrate-binding pocket in *Cc*EstA, *Pa*PBP and *Ec*AmpC forms a large tunnel, while in Lsa45, this tunnel is not observed [46,50]. Serine hydrolases have an enormous capacity to make major structural changes to suit different types of substrates. Conformational changes at the entrance to the substrate-binding pocket can be an important factor in recognition of more substrates, which sometimes lead to a promiscuous enzyme [60].

Structural studies have helped to identify similarities in the active site of enzymes of the α/β hydrolase family that acts in substrate catalysis [19,49,54,61]. Despite some differences, many of these similarities have been found in the structure of Lsa45. For example, the active site of Lsa45 has two of the three conserved motifs that have been identified in PBP [19], esterases [62,63], D-peptidase [49] and class C β-lactamases [50,64]. The motif I (S*xx*K) and motif II (Y*x*N) of α/β hydrolase family are conserved in Lsa45. Motif I is responsible for nucleophilic attack and is located at the α3-helix. In contrast, motif II is a short loop localized between the α9 and α10 helices forming one wall of the catalytic cavity which consists of a Y*x*N (class C β-lactamases) or S*x*N (class A β-lactamases) sequence motif [48]. Motif II in Lsa45 has the sequence ^{217}YSN^{219} with the residue Tyr217 pointing to catalytic serine (Ser122). Motif III (KTG-box) is common in class C β-lactamases and is not conserved in Lsa45; instead, the amino acid Gly is replaced by a Phe at the equivalent position (Fig. 3). This exchange may play an important steric role in regulating the entrance of substrates, allowing entry of less bulky substrates.

The classical catalytic triad signature responsible for the catalysis of α/β hydrolase is also present in Lsa45, localized in the substrate-binding pocket, where it is able to accommodate and react with its substrates. The catalytic triad is composed of the amino acids Ser122, Lys125 and Tyr217. It is predicted that these three residues in Lsa45 are essential in both β-lactamase and esterase activity. Like other members of the serine hydrolase family, Ser122

works as the probable nucleophile responsible for acetylation attacking the carbonyl carbon of lactam ring antibiotics and ester substrates. The role of Lys125 residue in catalysis depends on the enzyme. In class C β-lactamases, this residue stabilizes the oxyanion species, reducing the pKa of Tyr in the Y*x*N motif [65,66]. Lys125 and Tyr217, which are in close proximity to Ser122, are likely involved in deacetylation or deprotonation during catalysis [61]. Despite the low identity of the primary structure, the catalytic triad is highly conserved for different bacterial species (Figs. 3 and 4). The residues Ser122, Lys125, and Tyr217 of Lsa45 correspond to Ser64, Lys67, and Tyr150 of AmpC *E. coli*. In D-peptidase, these residues are represented by Ser74, Lys77, and Tyr17, while in EstU1 from an uncultured bacterium, the residues are located in Ser100, Lys103 and Tyr218 (Fig. 4).

Motif I is represented by the amino acids SVTK in Lsa45, SVSK in AmpC, SVTK in AD-peptidase and SMSK in EstU1. The three amino acids of motif II are YSN in Lsa45, YAN in AmpC, YSN in AD-peptidase and YGH in EstU1. The superposition of the active sites of the Lsa45 with other homolog enzymes is shown in Fig. 5. It reveals high similarity between the spatial orientation of residues of the active site of these enzymes. Therefore, it is clear that not only catalytic residues can directly influence the recognition and catalysis of different substrates (Fig. 5). In the case of Lsa45, the catalytic triad is conserved, but it may be that the overall substrate-binding pocket is suboptimal for the hydrolysis of β-lactam antibiotics. This was demonstrated for EstU1, which has weak β-lactam activity even though it possesses catalytic residues [61]. Despite exhibiting a range of activity as mentioned above, the mechanism of catalysis is practically the same for all these enzymes, with the cleavage of the amide bond. The exception is for enzymes that have esterase activity, in which case, catalysis is carboxylic ester hydrolysis.

3.2 Quaternary structure in solution

Lsa45 was purified and its oligomeric structure in solution was determined by SEC and SAXS. On SEC, Lsa45 had an elution profile with a single predominant peak consistent with a monomer of approximately 42 kDa (Fig. 6A). SAXS experiments were performed at 1 and 10 mg/mL concentrations. The primary analysis of the data suggests an aggregation tendency for the samples at 10 mg/mL, observed only for small values of *q*. For the subsequent analysis, a curve was generated by merging datasets from different concentrations: 1 mg/mL for small *q* values, and 10 mg/mL for higher *q* values. The radius of gyration (R_g) obtained by Guinier's approximation (Fig. 6B) was within the $q.Rg < 1.3$ limit and was in good agreement with R_g given by the *p(r)* method (Table 2). Fitting of the experimental data and *p(r)* adjustment (Fig. 6B–C) revealed a maximum diameter (D_{max}) of 69 Å. The simulated scattering of the crystallographic structure (Fig. 6D) yielded a D_{max} of 74.64 Å, suggesting a monomeric conformation of Lsa45 in solution. Molecular mass of the scattering molecule was calculated using SAXSMoW2 confirmed the monomeric state of Lsa45 with a discrepancy of 3.5% and with an experimental mass of 44.7 kDa compared with the theoretical mass of 46.3 kDa. In addition, the *dummy atoms* model (DAM) was generated based on the experimental data and its superimposition with the crystallographic structure (Fig. 6E and Fig. 7). These findings are further supported by the fact that there are no dimer interfaces for Lsa45 packed within the crystal, as defined by the program

PISA [67]. Thus, Lsa45 appears to be active as a monomer, and a similar behavior has been observed in other bifunctional PBP/esterase enzymes [46,68,69].

3.3 Structural similarity and evolution analyses

A total of 50 proteins with global structural similarity were found using Dali (Z-score >20), despite a low primary sequence identity between these proteins and Lsa45. Many of these structural homologs identified are active on a broad range of substrates, including nitrocefin, cephalothin, *p*-nitrophenyl esters, oxyimino, d-aminoacyl esters and cefotaxime. The range of possible substrates demonstrate the catalytic promiscuity of this class of enzymes, which has been discussed previously [70]. One of the possible reasons for the catalytic promiscuity of enzymes with α/β hydrolase fold may be due to the ability to mediate different catalytic mechanisms. The Dali server also revealed that Lsa45 structure is highly similar to 6-aminohexanoate-dimer hydrolase of *Flavobacterium sp*. with a Z-score of 31.8, RMSD 2.2 based on 292 of 384 C-alpha atoms and 21% sequence identity (PDB 1WYC). Another identified structure similar to Lsa45 was the EstU1, from an uncultured bacterium with a -score of 30.7, RMSD 2.4 based on 296 of 404 C-alpha atoms and 20% sequence identity (PDB 4IVI), which was also determined complexed with cephalothin, a first-generation cephalosporin antibiotic. EstU1 belongs to family VIII carboxylesterases, which displays β-lactamase activity against *p*-nitrophenyl esters. EstU1 has a β-lactamase-like topology and contains the residues Ser100, Lys103 and Tyr218, which correspond to the three catalytic residues of class C β-lactamases [61]. More distant structural homologs include putative β-lactamase of *Jeotgalibacillus marinus* - -score of 29.4, RMSD 2.6 based on 290 of 361 C-alpha atoms and 17% sequence identity (PDB 6KJJ); Est-Y29, a metagenomic homolog of the PBP/β-lactamase family with -score of 27.7, RMSD 2.5 based on 286 of 390 C-alpha atoms and 17% sequence identity (PDB 4P85); EstB from *Burkholderia gladioli*, an esterase with β-lactamase activity - -score of 27.1, RMSD 2.5 based on 280 of 377 C-alpha atoms and 18% sequence identity (PDB 1CI8); and AmpC from *E. coli* - -score of 26.1, RMSD 2.8 based on 287 of 361 C-alpha atoms and 18% sequence identity (PDB 3IWI).

Although there are a large number of structures with similar folds, we will focus on the structural comparison between Lsa45 and EstU1 from an uncultured bacterium [61] and AmpC from *E. coli*, because the two have esterase and β-lactamase activity [54], respectively, activities observed in Lsa45. The overall structure is very similar for these three enzymes but there are significant differences, mainly in the accessibility of the active site from the surrounding solvent. Evolutionary analyses were also performed using the DRCN method. The results in three sets of coevolving positions are shown in Fig. 8. The first set consists of residues D245, L198, P197, L125, G161 and P160 according to *E. coli* AmpC numbering (D226, L179, P178, L106, G142 e P141 in PDB 1FCM). The second set of coevolving residues are K83, S80 and Y166 in *E. coli* AMPC. Finally, there is a coevolving pair involving an aspartate and a tyrosine which is not present either in *E. coli* AmpC. One of the coevolving sets in the DRCN analysis has a very clear interpretation: K83, S80 and Y166 (*E. coli* AmpC) make up the catalytic triad in known β-lactamases [50], and Lsa45 has all three residues (Lys125, Ser122 and Tyr217 according to Uniprot numbering). What is notable in this overall coevolution pattern is the absence of coevolved residues directly related to specificity. In serine proteases, for example, besides a coevolving set including

the catalytic triad coevolves and other residues in the active site, there is a coevolving pair specific to trypsins and coevolution signal for the residues forming the auxiliary triad in some serine proteases [71]. For this protein family, however, the catalytic triad does not show significant coevolution with other residues, and the six-residue group mentioned above is scattered around the structure. Two interpretations are possible: either the variety of specificities in this protein family is so high that possible coevolving residues for specific sub-classes have diluted correlation signals, or there are no such patterns for members of this protein family. While the two interpretations are not mutually exclusive, the second is in agreement with the prevalence of promiscuous enzymes in this protein family.

3.4 Penicillin binding assay and enzymatic kinetics

Bocillin FL penicillin was used to probe the interaction between Lsa45 and β-lactams. This dye has been used to characterize PBPs and -lactamases [72,73]. Fig. 9 shows SDS-PAGE of binding of Bocillin FL with Lsa45 in a concentration-dependent manner. As the concentration of Bocillin FL increases, and the intensity of the bands in the gel also increases. This data suggests that Bocillin FL covalently binds to Lsa45, possibly through the formation of an acylated complex. Although binding occurs, we observe that binding is extremely weak when compared to other PBPs[39,74,75].

The hydrolytic activity of Lsa45 was examined using nitrocefin and *p*-NPA (Fig. 10A). Nitrocefin, once hydrolyzed, rapidly changes color from yellow to red. Lsa45 showed β-lactamase activity against nitrocefin. The substrate *p*-NPA was also used to test for esterase activity (Fig. 10B). The esterase activity of Lsa45 converted *p*-NPA (colorless) to *p*-nitrophenol (yellow). Similarly, other bifunctional β-lactamase/esterase enzymes such as *Lg*LacI [76], EstA [70] and *Cc*EstA [46] showed activities for β-lactams and *p*-nitrophenyl esters. Three different temperatures and several protein concentrations were tested to choose the ideal parameters for kinetic enzymatic assays. For both substrates, 37 °C was chosen as the temperature, with 50 μg of protein for nitrocefin and 25 μg for *p*-NPA.

Fig. 10C shows the Michaelis-Menten plot for Lsa45 activity with nitrocefin and *p*-NPA, respectively. The kinetic parameters of Lsa45 for nitrocefin and *p*-NPA were determined and are summarized in Table 3. All the kinetic parameters are very similar between the two substrates. The K_m values for nitrocefin (235.0 μM) and *p*-NPA (849.3 μM) were determined to be within a similar range. The k_{cat} value for *p*-NPA was only one order of magnitude higher than those for nitrocefin, with values of 0.668 s^{-1} for *p*-NPA and 0.040 s^{-1} for nitrocefin. The catalytic efficiencies (k_{cat}/K_m) for both substrates were low, with values of 0.17 $mM^{-1}s^{-1}$ for nitrocefin and slightly higher for p-NPA, 0.786 mM-1s-1. The weak catalysis and specificity of promiscuous enzymes with β-lactamase should be related to the substrate-binding pocket since the pocket is not optimized for either activity [61,72]. Most of them have bifunctional β-lactamase/esterase activity and use the same substrate-binding pocket to hydrolyze substrates [46,56,62,76]. Others, like the bifunctional enzyme Tp47 from the spirochete Treponema palladium has β-lactamase and carboxypeptidase activities [72].

The kinetic findings for Lsa45 differ from a recent report by Ryu and colleagues who studied a similar protein, *Cc*EstA from *C. crescentus*, which was more efficient for *p*-

nitrophenyl esters than nitrocefin [46]. In another kinetic study, this time of EstU1, the ester *p*-nitrophenyl butyrate and β-lactam cefazolin had the same affinity for EstU1, but the turnover efficiency of cefazolin was much lower [63]. The enzyme EstSRT1 has the same behavior as EstU1, with higher catalytic efficiency for *p*-nitrophenyl butyrate and lower for β-lactams [62]. Another enzyme that behaves differently from Lsa45 is EstC, which was identified from culture-independent metagenomic sequencing. EstC also has weak β-lactamase activity against nitrocefin. Substrate specificity studies showed that EstC prefers short to medium acyl chain length of *p*-nitrophenyl esters [56]. Therefore, it was observed that unlike other similar enzymes that have a preferential esterase activity, Lsa45 demonstrated more balanced kinetic parameters for both activities. However, it was observed that β-lactam hydrolysis is relatively weak for the cases shown.

4. Conclusions

Here, the first structure of a bifunctional PBP/esterase (Lsa45) of *L. interrogans* was determined and the protein was characterized biochemically. The structure and solution studies provided evidence that Lsa45 is a monomer. Based on sequence and structure alignments, it was possible to suggest the region of the catalytic binding site. This region contains the catalytic triad formed by the amino acids Ser122, Lys125 and Tyr217, which are essential for β-lactamase and esterase catalysis. In addition to structural studies, Lsa45 showed a binding to Bocillin FL, a dye analog of penicillin V that has been used to determine PBP and β-lactamase profiles of enzymes belonging to different bacteria. Finally, we demonstrated that Lsa45 is capable of hydrolyzing the β-lactam antibiotic nitrocefin and ester *p*-NPA. Nevertheless, kinetic studies revealed that Lsa45 was more efficient at degrading *p*-NPA as compared to nitrocefin. Although the structure and activity of Lsa45 were revealed in this study, its physiological function in the bacterium still needs to be explored. All these characteristics identified for Lsa45 have paved the way to understand the mechanism of this enzyme as well as to help design new therapeutic strategies through the prevention performing a structural mapping of epitopes, since Lsa45 is a leptospiral surface adhesin or in the treatment of leptospirosis using Lsa45 as a target for design new inhibitors. However, for a better understand of the role molecular of this enzyme in *L. interrogans* bacteria, further functional and structural studies should be carried out, such as site-directed mutagenesis, new kinetic assays with other substrates or even in vivo assays.

Acknowledgments

The authors are grateful to all the members for their support of this project. We thank L. Spiegelman for providing Esp. The Brazilian agencies FAPESP (Grants 2014/50981-0; 2019/17488-2), CNPq (Grants 301229/2017-1; 304445/2021-5), and Fundacao Butantan financially supported this work; Jademilson C. Santos (2018/20321-0 and 2017/25167-6) and Luis G. V. Fernandes have postdoctoral fellowships from FAPESP (2017/06731-8). SH and PG were supported by NIH R56 AI096837. LNLS, Robolab and LNBIO facilities.

References

[1]. Adler B, de la Peña Moctezuma A, Leptospira and leptospirosis, Vet Microbiol. 140 (2010) 287–296. 10.1016/j.vetmic.2009.03.012. [PubMed: 19345023]

[2]. Haake DA, Dundoo M, Cader R, Kubak BM, Hartskeerl RA, Sejvar JJ, Ashford DA, Leptospirosis, Water Sports, and Chemoprophylaxis, Clinical Infectious Diseases. 34 (2002) e40–e43. 10.1086/339942. [PubMed: 11941571]

[3]. Hartskeerl RA, Collares-Pereira M, Ellis WA, Emergence, control and re-emerging leptospirosis: dynamics of infection in the changing world, Clinical Microbiology and Infection. 17 (2011) 494–501. 10.1111/j.1469-0691.2011.03474.x. [PubMed: 21414083]

[4]. Rajapakse S, Leptospirosis: clinical aspects, Clinical Medicine. 22 (2022) 14–17. 10.7861/clinmed.2021-0784.

[5]. Bharti AR, Nally JE, Ricaldi JN, Matthias MA, Diaz MM, Lovett MA, Levett PN, Gilman RH, Willig MR, Gotuzzo E, Vinetz JM, Leptospirosis: a zoonotic disease of global importance, Lancet Infect Dis. 3 (2003) 757–771. 10.1016/S1473-3099(03)00830-2. [PubMed: 14652202]

[6]. Bajani MD, Ashford DA, Bragg SL, Woods CW, Aye T, Spiegel RA, Plikaytis BD, Perkins BA, Phelan M, Levett PN, Weyant RS, Evaluation of Four Commercially Available Rapid Serologic Tests for Diagnosis of Leptospirosis, J Clin Microbiol. 41 (2003) 803–809. 10.1128/JCM.41.2.803-809.2003. [PubMed: 12574287]

[7]. Turner LH, Leptospirosis III. Maintenance, isolation and demonstration of leptospires, Trans R Soc Trop Med Hyg. 64 (1970) 623–646. 10.1016/0035-9203(70)90087-8. [PubMed: 4098633]

[8]. Hornsby RL, Alt DP, Nally JE, Isolation and propagation of leptospires at 37 °C directly from the mammalian host, Sci Rep. 10 (2020) 9620. 10.1038/S41598-020-66526-4. [PubMed: 32541841]

[9]. Goris MGA, Hartskeerl RA, Leptospirosis Serodiagnosis by the Microscopic Agglutination Test, Curr Protoc Microbiol. 32 (2014) 12E.5.1–12E.5.18. 10.1002/9780471729259.MC12E05S32.

[10]. Levett PN, Branch SL, Whittington CU, Edwards CN, Paxton H, Two methods for rapid serological diagnosis of acute leptospirosis, Am Soc Microbiol. 8 (2001) 349–351. 10.1128/CDLI.8.2.349-351.2001.

[11]. Watt G, Linda Tuazon M, Santiago E, Padre LP, Calubaquib C, Ranoa CP, Laughlin LW, PLACEBO-CONTROLLED TRIAL OF INTRAVENOUS PENICILLIN FOR SEVERE AND LATE LEPTOSPIROSIS, The Lancet. 331 (1988) 433–435. 10.1016/S0140-6736(88)91230-5.

[12]. Brett-Major DM, Coldren R, Antibiotics for leptospirosis, Cochrane Database of Systematic Reviews. (2012). 10.1002/14651858.CD008264.PUB2/ABSTRACT.

[13]. Griffith ME, Hospenthal DR, Murray CK, Antimicrobial therapy of leptospirosis, Curr Opin Infect Dis. 19 (2006) 533–537. 10.1097/QCO.0B013E3280106818. [PubMed: 17075327]

[14]. Charan J, Saxena D, … S.M.-I. journal of, undefined 2013, Antibiotics for the treatment of leptospirosis: systematic review and meta-analysis of controlled trials, Ncbi.Nlm.Nih.Gov. (n.d.). https://www.ncbi.nlm.nih.gov/pmc/articles/PMC3733179/

[15]. Guzmán Pérez M, Blanch Sancho J. Javier, Segura Luque J. Carlos, Mateos Rodriguez F, Martínez Alfaro E, Solís García del Pozo J, Pérez G, Sancho B, Luque S, Rodriguez M, Alfaro M, García del Pozo S, Current Evidence on the Antimicrobial Treatment and Chemoprophylaxis of Human Leptospirosis: A Meta-Analysis, Mdpi.Com. 10 (2021). 10.3390/pathogens10091125.

[16]. Harris BM, Blatz PJ, Hinkle MK, McCall S, Beckius ML, Mende K, Robertson JL, Griffith ME, Murray CK, Hospenthal DR, In vitro and in vivo activity of first generation cephalosporins against Leptospira, American Journal of Tropical Medicine and Hygiene. 85 (2011) 905–908. 10.4269/AJTMH.2011.11-0352. [PubMed: 22049047]

[17]. Zhang W, Zhang N, Wang W, Wang F, Gong Y, Jiang H, Zhang Z, Liu X, Song X, Wang T, Ding Z, Cao Y, Efficacy of cefepime, ertapenem and norfloxacin against leptospirosis and for the clearance of pathogens in a hamster model, Microb Pathog. 77 (2014) 78–83. 10.1016/J.MICPATH.2014.11.006. [PubMed: 25450882]

[18]. Macheboeuf P, Contreras-Martel C, Job V, Dideberg O, Dessen A, Penicillin binding proteins: Key players in bacterial cell cycle and drug resistance processes, FEMS Microbiol Rev. 30 (2006) 673–691. 10.1111/J.1574-6976.2006.00024.X. [PubMed: 16911039]

[19]. Ngo TD, Ryu BH, Ju H, Jang EJ, Kim KK, Kim TD, Crystallographic analysis and biochemical applications of a novel penicillin-binding protein/β-lactamase homologue from a metagenomic library, Acta Crystallogr D Biol Crystallogr. 70 (2014) 2455–2466. 10.1107/S1399004714015272. [PubMed: 25195758]

[20]. Fernandes LG, Siqueira GH, Teixeira ARF, Silva LP, Figueredo JM, Cosate MR, Vieira ML, Nascimento ALTO, Leptospira spp.: Novel insights into host–pathogen interactions, Vet Immunol Immunopathol. 176 (2016) 50–57. 10.1016/j.vetimm.2015.12.004. [PubMed: 26727033]

[21]. Daroz BB, Fernandes L.G. v., Cavenague MF, Kochi LT, Passalia FJ, Takahashi MB, Nascimento Filho EG, Teixeira AF, Nascimento ALTO, A Review on Host-Leptospira Interactions: What We Know and Future Expectations, Front Cell Infect Microbiol. 11 (2021). 10.3389/fcimb.2021.777709.

[22]. Fernandes L.G. v., Vieira ML, Alves IJ, de Morais ZM, Vasconcellos SA, Romero EC, Nascimento ALTO, Functional and immunological evaluation of two novel proteins of Leptospira spp., Microbiology (N Y). 160 (2014) 149–164. 10.1099/mic.0.072074-0.

[23]. Abendroth J, Gardberg AS, Robinson JI, Christensen JS, Staker BL, Myler PJ, Stewart LJ, Edwards TE, SAD phasing using iodide ions in a high-throughput structural genomics environment, J Struct Funct Genomics. 12 (2011) 83–95. 10.1007/s10969-011-9101-7. [PubMed: 21359836]

[24]. Dauter Z, Dauter M, Rajashankar KR, Novel approach to phasing proteins: derivatization by short cryo-soaking with halides, Acta Crystallogr D Biol Crystallogr. 56 (2000) 232–237. 10.1107/S0907444999016352. [PubMed: 10666615]

[25]. Kabsch W, XDS, Acta Crystallogr D Biol Crystallogr. 66 (2010) 125–132. 10.1107/S0907444909047337. [PubMed: 20124692]

[26]. Evans PR, Murshudov GN, How good are my data and what is the resolution?, Acta Crystallogr D Biol Crystallogr. 69 (2013) 1204–1214. 10.1107/S0907444913000061. [PubMed: 23793146]

[27]. Terwilliger TC, Adams PD, Read RJ, McCoy AJ, Moriarty NW, Grosse-Kunstleve RW, Afonine P. v., Zwart PH, Hung L-W, Decision-making in structure solution using Bayesian estimates of map quality: the *PHENIX AutoSol* wizard, Acta Crystallogr D Biol Crystallogr. 65 (2009) 582–601. 10.1107/S0907444909012098. [PubMed: 19465773]

[28]. Terwilliger TC, Grosse-Kunstleve RW, Afonine P. v., Moriarty NW, Zwart PH, Hung L-W, Read RJ, Adams PD, Iterative model building, structure refinement and density modification with the *PHENIX AutoBuild* wizard, Acta Crystallogr D Biol Crystallogr. 64 (2008) 61–69. 10.1107/S090744490705024X. [PubMed: 18094468]

[29]. Adams PD, Grosse-Kunstleve RW, Hung L-W, Ioerger TR, McCoy AJ, Moriarty NW, Read RJ, Sacchettini JC, Sauter NK, Terwilliger TC, *PHENIX* : building new software for automated crystallographic structure determination, Acta Crystallogr D Biol Crystallogr. 58 (2002) 1948–1954. 10.1107/S0907444902016657. [PubMed: 12393927]

[30]. Emsley P, Cowtan K, *Coot* : model-building tools for molecular graphics, Acta Crystallogr D Biol Crystallogr. 60 (2004) 2126–2132. 10.1107/S0907444904019158. [PubMed: 15572765]

[31]. Chen VB, Arendall WB, Headd JJ, Keedy DA, Immormino RM, Kapral GJ, Murray LW, Richardson JS, Richardson DC, *MolProbity* : all-atom structure validation for macromolecular crystallography, Acta Crystallogr D Biol Crystallogr. 66 (2010) 12–21. 10.1107/S0907444909042073. [PubMed: 20057044]

[32]. Joosten RP, Long F, Murshudov GN, Perrakis A, The *PDB_REDO* server for macromolecular structure model optimization, IUCrJ. 1 (2014) 213–220. 10.1107/S2052252514009324.

[33]. Delano DW, PyMOL molecular graphics system, (2002).

[34]. Holm L, Rosenström P, Dali server: conservation mapping in 3D, Nucleic Acids Res. 38 (2010) W545–W549. 10.1093/nar/gkq366. [PubMed: 20457744]

[35]. Yu J, Zhou Y, Tanaka I, Yao M, Roll: a new algorithm for the detection of protein pockets and cavities with a rolling probe sphere, Bioinformatics. 26 (2010) 46–52. 10.1093/bioinformatics/btp599. [PubMed: 19846440]

[36]. Hammersley AP, *FIT2D* : a multi-purpose data reduction, analysis and visualization program, J Appl Crystallogr. 49 (2016) 646–652. 10.1107/S1600576716000455.

[37]. Svergun DI, Restoring Low Resolution Structure of Biological Macromolecules from Solution Scattering Using Simulated Annealing, Biophys J. 76 (1999) 2879–2886. 10.1016/S0006-3495(99)77443-6. [PubMed: 10354416]

[38]. Piiadov V, Ares de Araújo E, Oliveira Neto M, Craievich AF, Polikarpov I, SAXSMoW 2.0: Online calculator of the molecular weight of proteins in dilute solution from experimental SAXS data measured on a relative scale, Protein Science. 28 (2019) 454–463. 10.1002/pro.3528. [PubMed: 30371978]

[39]. Zhao G, Meier TI, Kahl SD, Gee KR, Blaszczak LC, BOCILLIN FL, a Sensitive and Commercially Available Reagent for Detection of Penicillin-Binding Proteins, Antimicrob Agents Chemother. 43 (1999) 1124–1128. 10.1128/AAC.43.5.1124. [PubMed: 10223924]

[40]. Spiegelman L, Bahn-Suh A, Montaño ET, Zhang L, Hura GL, Patras KA, Kumar A, Tezcan FA, Nizet V, Tsutakawa SE, Ghosh P, Strengthening of enterococcal biofilms by Esp, PLoS Pathog. 18 (2022) e1010829. 10.1371/journal.ppat.1010829. [PubMed: 36103556]

[41]. O'Callaghan CH, Morris A, Kirby SM, Shingler AH, Novel Method for Detection of β-Lactamases by Using a Chromogenic Cephalosporin Substrate, Antimicrob Agents Chemother. 1 (1972) 283–288. 10.1128/AAC.1.4.283. [PubMed: 4208895]

[42]. Bleicher L, Lemke N, Garratt RC, Using Amino Acid Correlation and Community Detection Algorithms to Identify Functional Determinants in Protein Families, PLoS One. 6 (2011) e27786. 10.1371/journal.pone.0027786. [PubMed: 22205928]

[43]. Fonseca-Júnior NJ, Afonso MQL, Oliveira LC, Bleicher L, PFstats: A Network-Based Open Tool for Protein Family Analysis, Journal of Computational Biology. 25 (2018) 480–486. 10.1089/cmb.2017.0181. [PubMed: 29481292]

[44]. Finn RD, Bateman A, Clements J, Coggill P, Eberhardt RY, Eddy SR, Heger A, Hetherington K, Holm L, Mistry J, Sonnhammer ELL, Tate J, Punta M, Pfam: the protein families database, Nucleic Acids Res. 42 (2014) D222–D230. 10.1093/nar/gkt1223. [PubMed: 24288371]

[45]. Matthews BW, Solvent content of protein crystals, J Mol Biol. 33 (1968) 491–497. 10.1016/0022-2836(68)90205-2. [PubMed: 5700707]

[46]. Ryu BH, Ngo TD, Yoo W, Lee S, Kim B-Y, Lee E, Kim KK, Kim TD, Biochemical and Structural Analysis of a Novel Esterase from Caulobacter crescentus related to Penicillin-Binding Protein (PBP), Sci Rep. 6 (2016) 37978. 10.1038/srep37978. [PubMed: 27905486]

[47]. Bulach DM, Zuerner RL, Wilson P, Seemann T, McGrath A, Cullen PA, Davis J, Johnson M, Kuczek E, Alt DP, Peterson-Burch B, Coppel RL, Rood JI, Davies JK, Adler B, Genome reduction in *Leptospira borgpetersenii* reflects limited transmission potential, Proceedings of the National Academy of Sciences. 103 (2006) 14560–14565. 10.1073/pnas.0603979103.

[48]. Wagner UG, Petersen EI, Schwab H, Kratky C, EstB from Burkholderia gladioli: A novel esterase with a β-lactamase fold reveals steric factors to discriminate between esterolytic and β-lactam cleaving activity, Protein Science. 11 (2009) 467–478. 10.1110/ps.33002.

[49]. Nakano S, Okazaki S, Ishitsubo E, Kawahara N, Komeda H, Tokiwa H, Asano Y, Structural and computational analysis of peptide recognition mechanism of class-C type penicillin binding protein, alkaline D-peptidase from Bacillus cereus DF4-B, Sci Rep. 5 (2015) 13836. 10.1038/srep13836. [PubMed: 26370172]

[50]. Usher KC, Blaszczak LC, Weston GS, Shoichet BK, Remington SJ, Three-Dimensional Structure of AmpC β-Lactamase from *Escherichia c oli* Bound to a Transition-State Analogue: Possible Implications for the Oxyanion Hypothesis and for Inhibitor Design, Biochemistry. 37 (1998) 16082–16092. 10.1021/bi981210f. [PubMed: 9819201]

[51]. Carugo O, How large B-factors can be in protein crystal structures, BMC Bioinformatics. 19 (2018) 61. 10.1186/s12859-018-2083-8. [PubMed: 29471780]

[52]. Otero LH, Rojas-Altuve A, Llarrull LI, Carrasco-López C, Kumarasiri M, Lastochkin E, Fishovitz J, Dawley M, Hesek D, Lee M, Johnson JW, Fisher JF, Chang M, Mobashery S, Hermoso JA, How allosteric control of *Staphylococcus aureus* penicillin binding protein 2a enables methicillin resistance and physiological function, Proceedings of the National Academy of Sciences. 110 (2013) 16808–16813. 10.1073/pnas.1300118110.

[53]. Ruble JF, Lefurgy ST, Cornish VW, Powers RA, Structural analysis of the Asn152Gly mutant of P99 cephalosporinase, Acta Crystallogr D Biol Crystallogr. 68 (2012) 1189–1193. 10.1107/S0907444912024080. [PubMed: 22948919]

[54]. Thomas VL, McReynolds AC, Shoichet BK, Structural Bases for Stability–Function Tradeoffs in Antibiotic Resistance, J Mol Biol. 396 (2010) 47–59. 10.1016/j.jmb.2009.11.005. [PubMed: 19913034]

[55]. Lahiri SD, Mangani S, Durand-Reville T, Benvenuti M, de Luca F, Sanyal G, Docquier J-D, Structural Insight into Potent Broad-Spectrum Inhibition with Reversible Recyclization Mechanism: Avibactam in Complex with CTX-M-15 and Pseudomonas aeruginosa AmpC

β-Lactamases, Antimicrob Agents Chemother. 57 (2013) 2496–2505. 10.1128/AAC.02247-12. [PubMed: 23439634]

[56]. Rashamuse K, Magomani V, Ronneburg T, Brady D, A novel family VIII carboxylesterase derived from a leachate metagenome library exhibits promiscuous β-lactamase activity on nitrocefin, Appl Microbiol Biotechnol. 83 (2009) 491–500. 10.1007/s00253-009-1895-x. [PubMed: 19190902]

[57]. Rashamuse KJ, Burton SG, Stafford WHL, Cowan DA, Molecular Characterization of a Novel Family VIII Esterase from *Burkholderia multivorans* UWC10, Microb Physiol. 13 (2007) 181–188. 10.1159/000103610.

[58]. Mokoena N, Mathiba K, Tsekoa T, Steenkamp P, Rashamuse K, Functional characterisation of a metagenome derived family VIII esterase with a deacetylation activity on β-lactam antibiotics, Biochem Biophys Res Commun. 437 (2013) 342–348. 10.1016/j.bbrc.2013.06.076. [PubMed: 23827391]

[59]. McDonough MA, Anderson JW, Silvaggi NR, Pratt RF, Knox JR, Kelly JA, Structures of Two Kinetic Intermediates Reveal Species Specificity of Penicillin-binding Proteins, J Mol Biol. 322 (2002) 111–122. 10.1016/S0022-2836(02)00742-8. [PubMed: 12215418]

[60]. Zou T, Risso VA, Gavira JA, Sanchez-Ruiz JM, Ozkan SB, Evolution of Conformational Dynamics Determines the Conversion of a Promiscuous Generalist into a Specialist Enzyme, Mol Biol Evol. 32 (2015) 132–143. 10.1093/molbev/msu281. [PubMed: 25312912]

[61]. Cha S-S, An YJ, Jeong C-S, Kim M-K, Jeon JH, Lee C-M, Lee HS, Kang SG, Lee J-H, Structural basis for the β-lactamase activity of EstU1, a family VIII carboxylesterase, Proteins: Structure, Function, and Bioinformatics. 81 (2013) 2045–2051. 10.1002/prot.24334.

[62]. Jeon JH, Lee HS, Lee JH, Koo B-S, Lee C-M, Lee SH, Kang SG, Lee J-H, A novel family VIII carboxylesterase hydrolysing third- and fourth-generation cephalosporins, Springerplus. 5 (2016) 525. 10.1186/s40064-016-2172-y. [PubMed: 27186489]

[63]. Jeon JH, Kim S-J, Lee HS, Cha S-S, Lee JH, Yoon S-H, Koo B-S, Lee C-M, Choi SH, Lee SH, Kang SG, Lee J-H, Novel Metagenome-Derived Carboxylesterase That Hydrolyzes β-Lactam Antibiotics, Appl Environ Microbiol. 77 (2011) 7830–7836. 10.1128/AEM.05363-11. [PubMed: 21908637]

[64]. Powers RA, Swanson HC, Taracila MA, Florek NW, Romagnoli C, Caselli E, Prati F, Bonomo RA, Wallar BJ, Biochemical and Structural Analysis of Inhibitors Targeting the ADC-7 Cephalosporinase of *Acinetobacter baumannii*, Biochemistry. 53 (2014) 7670–7679. 10.1021/bi500887n. [PubMed: 25380506]

[65]. Chen Y, McReynolds A, Shoichet BK, Re-examining the role of Lys67 in class C β-lactamase catalysis, Protein Science. (2009) NA-NA. 10.1002/pro.60.

[66]. Dalal V, Kumar P, Rakhaminov G, Qamar A, Fan X, Hunter H, Tomar S, Golemi-Kotra D, Kumar P, Repurposing an Ancient Protein Core Structure: Structural Studies on FmtA, a Novel Esterase of Staphylococcus aureus, J Mol Biol. 431 (2019) 3107–3123. 10.1016/j.jmb.2019.06.019. [PubMed: 31260692]

[67]. Krissinel E, Henrick K, Inference of Macromolecular Assemblies from Crystalline State, J Mol Biol. 372 (2007) 774–797. 10.1016/j.jmb.2007.05.022. [PubMed: 17681537]

[68]. Jeong J-H, Kim Y-S, Rojviriya C, Ha S-C, Kang BS, Kim Y-G, Crystal Structures of Bifunctional Penicillin-Binding Protein 4 from Listeria monocytogenes, Antimicrob Agents Chemother. 57 (2013) 3507–3512. 10.1128/AAC.00144-13. [PubMed: 23669378]

[69]. Okazaki S, Suzuki A, Komeda H, Yamaguchi S, Asano Y, Yamane T, Crystal Structure and Functional Characterization of a D-Stereospecific Amino Acid Amidase from Ochrobactrum anthropi SV3, a New Member of the Penicillin-recognizing Proteins, J Mol Biol. 368 (2007) 79–91. 10.1016/j.jmb.2006.10.070. [PubMed: 17331533]

[70]. Wagner UG, DiMaio F, Kolkenbrock S, Fetzner S, Crystal structure analysis of EstA from *Arthrobacter* sp. Rue61a - an insight into catalytic promiscuity, FEBS Lett. 588 (2014) 1154–1160. 10.1016/j.febslet.2014.02.045. [PubMed: 24613918]

[71]. Querino Lima Afonso M, da Fonseca NJ, de Oliveira LC, Lobo FP, Bleicher L, Coevolved Positions Represent Key Functional Properties in the Trypsin-Like Serine Proteases Protein

Family, J Chem Inf Model. 60 (2020) 1060–1068. 10.1021/acs.jcim.9b00903. [PubMed: 31895561]

[72]. Cha JY, Ishiwata A, Mobashery S, A Novel β-Lactamase Activity from a Penicillin-binding Protein of Treponema pallidum and Why Syphilis Is Still Treatable with Penicillin, Journal of Biological Chemistry. 279 (2004) 14917–14921. 10.1074/jbc.M400666200. [PubMed: 14747460]

[73]. Pal S, Ghosh AS, PBP Isolation and DD-Carboxypeptidase Assay, in: 2019: pp. 207–225. 10.1007/978-1-4939-9118-1_20.

[74]. Fan X, Liu Y, Smith D, Konermann L, Siu KWM, Golemi-Kotra D, Diversity of Penicillin-binding Proteins, Journal of Biological Chemistry. 282 (2007) 35143–35152. 10.1074/jbc.M706296200. [PubMed: 17925392]

[75]. Sutaria DS, Moya B, Green KB, Kim TH, Tao X, Jiao Y, Louie A, Drusano GL, Bulitta JB, First Penicillin-Binding Protein Occupancy Patterns of β-Lactams and β-Lactamase Inhibitors in Klebsiella pneumoniae, Antimicrob Agents Chemother. 62 (2018). 10.1128/AAC.00282-18.

[76]. Le LTHL, Yoo W, Wang Y, Jeon S, Kim KK, Kim H-W, Kim TD, Dual functional roles of a novel bifunctional β-lactamase/esterase from Lactococcus garvieae, Int J Biol Macromol. 206 (2022) 203–212. 10.1016/j.ijbiomac.2022.02.081. [PubMed: 35183603]

HIGHLIGHTS

- Leptospiral surface adhesin 45kDa (Lsa45) is active as monomer in solution.
- Lsa45 showed β-lactamase and esterase activities.
- Lsa45 structure from was determined to 1.62 Å resolution.
- Lsa45 structure revealed a large α/β domain and a small α-helix domain.

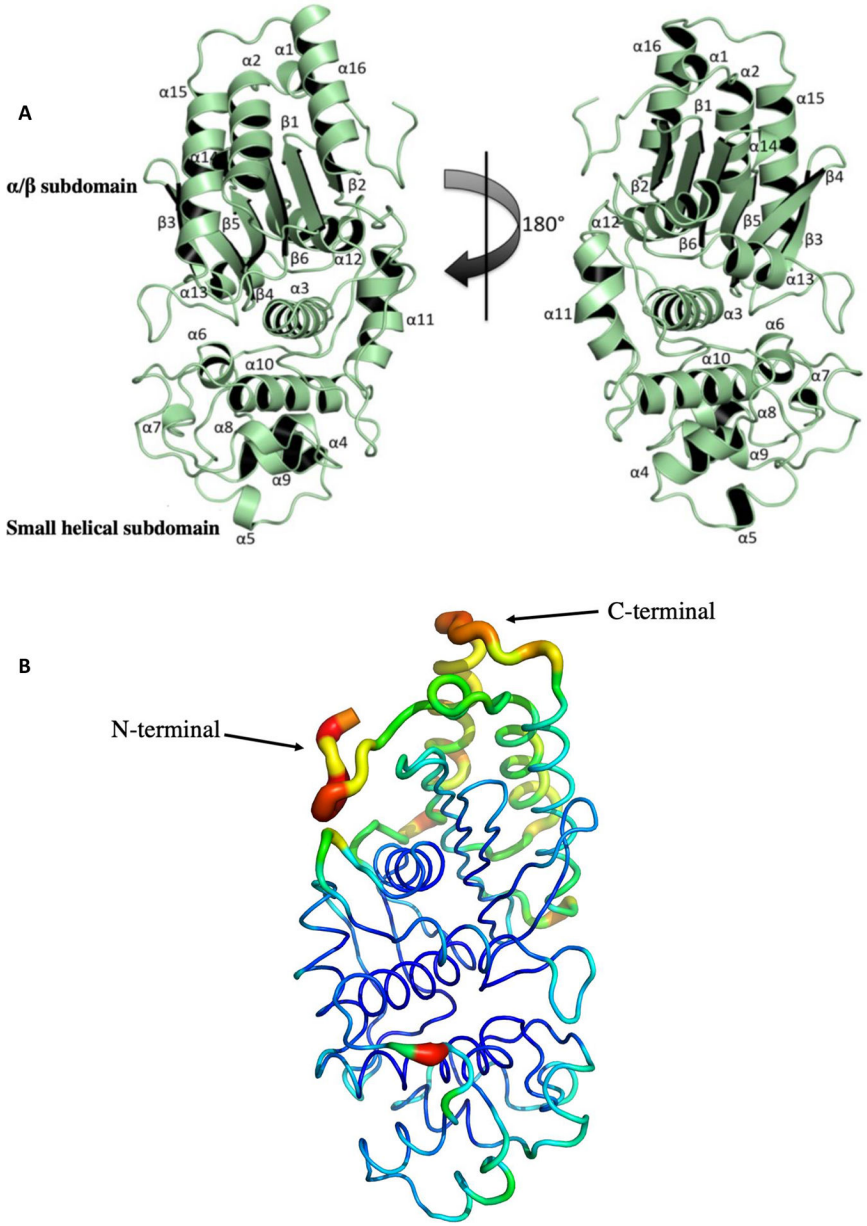

Figure 1.

The overall crystal structure of Leptospiral surface adhesin of 45 kDa (Lsa45). A) The structure of Lsa45 is a monomer with two subdomains. The upper part of the structure in the orientation depicted is an α/β hydrolase-like subdomain and the bottom a smaller α-helical subdomain. B) *B*-factor demonstration of the Lsa45 colored by *B*-factor value. The protein is shown as a putty representation, as implemented by PyMOL. The residues have low blue and green, while the residues with high *B*-factor values are colored by yellow to red.

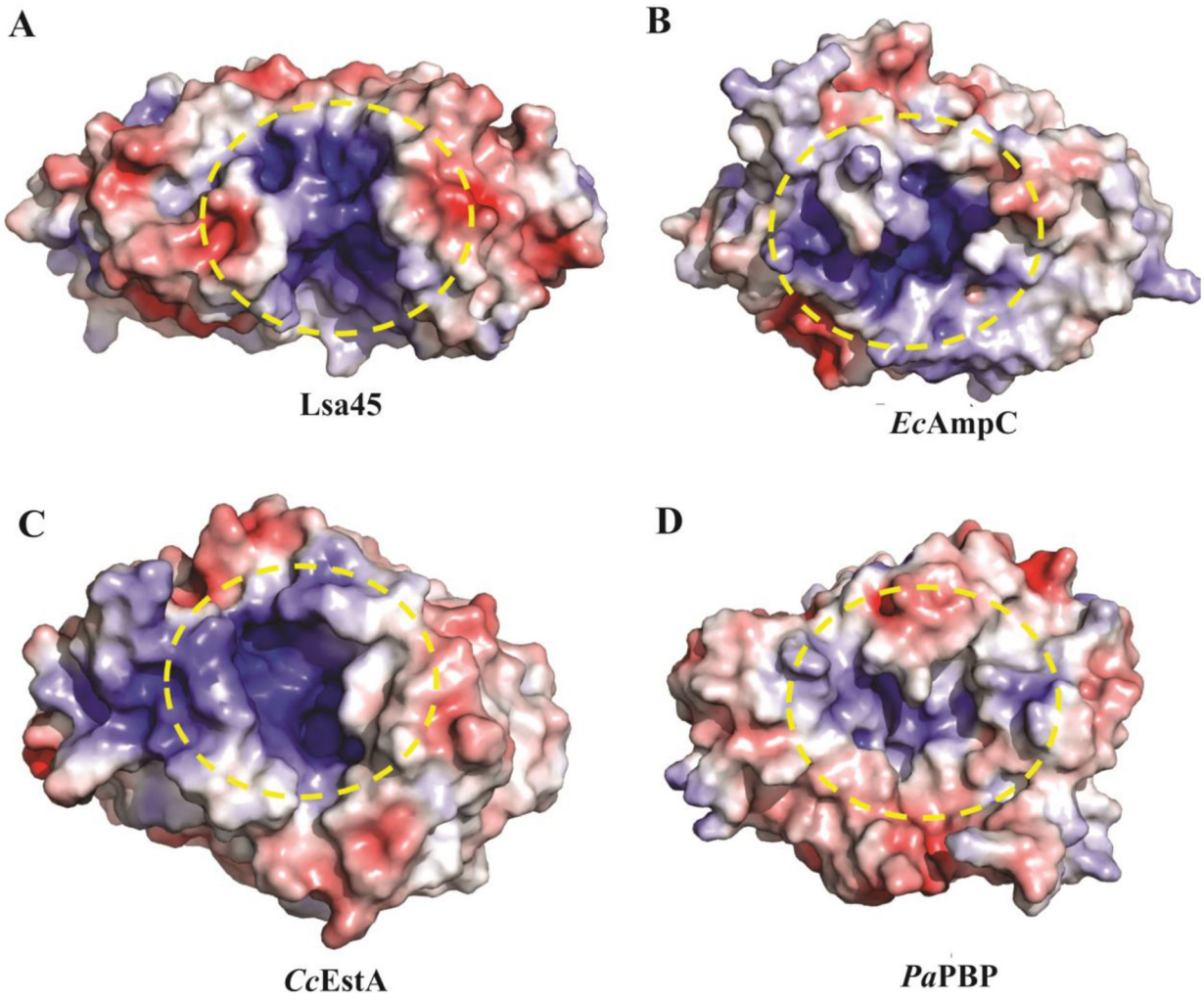

Figure 2.

Molecular surface analyses of Lsa45. All molecular surfaces were calculated using APBS Electrostatics Plugin into PyMOL. A) The yellow dashed circle shows the substrate binding pocket of Lsa45, B) *Escherichia coli* AmpC (*Ec*AmpC), C) *Caulobacter crescentus* (*Cc*EstA) and D) *Pyrococcus abyssi* (*Pa*PBP). Blue, red, and white colors indicate positively charged, negatively charged, and hydrophobic surfaces, respectively.

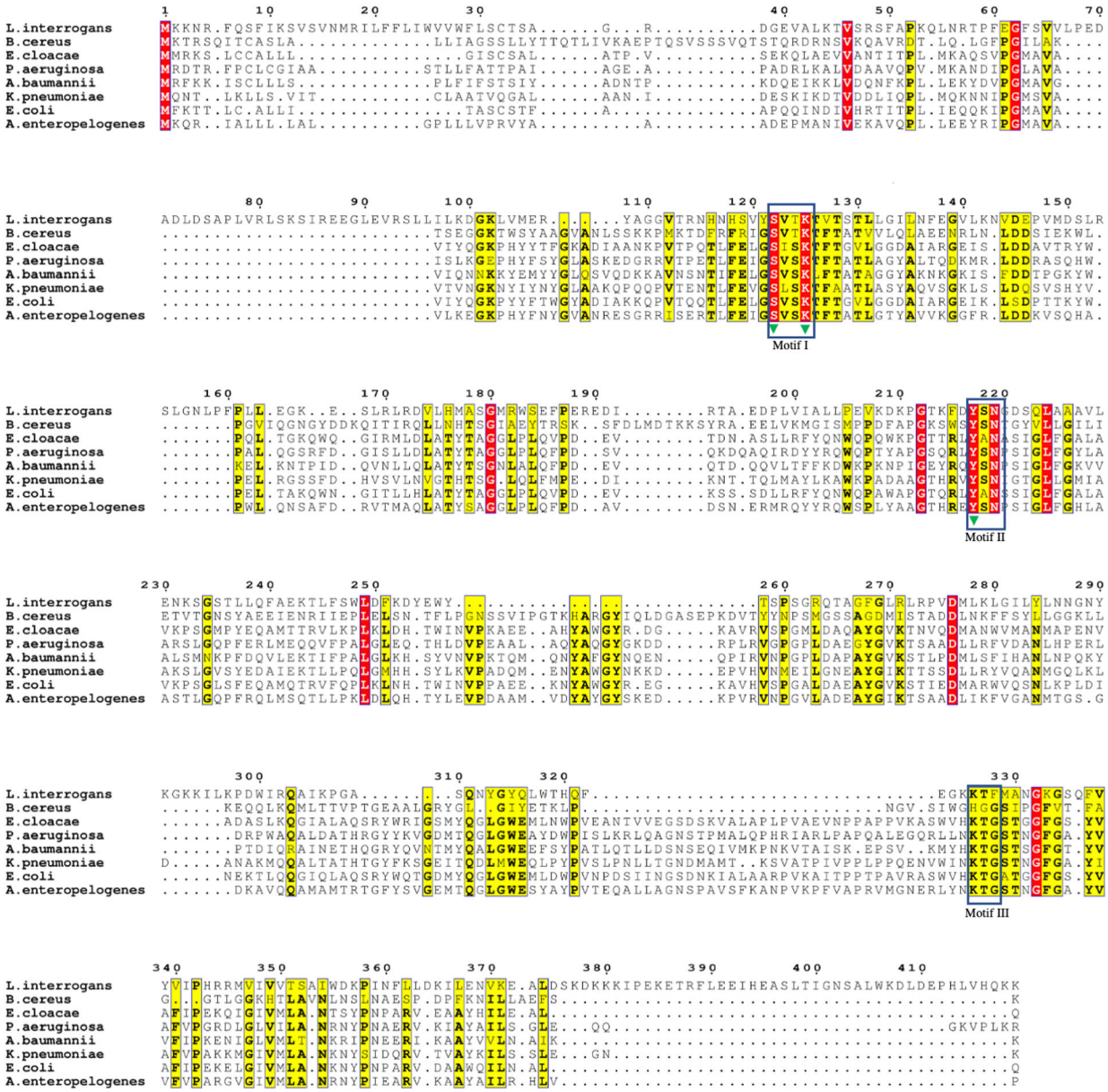

Figure 3.

Multiple sequence alignment of Lsa45 with several serine hydrolases. Similar residues are colored in yellow and more conserved residues are in red. Numbers correspond to the Lsa45 sequence. The rectangles show the motifs and green triangles correspond to catalytic triad amino acids in the active site of Lsa45. Lsa45 (UniProtKB: Q72UC8), Alkaline D-peptidase - *Bacillus cereus* (UniProtKB: P94288), AmpC - *Pseudomonas aeruginosa* (UniProtKB: Q541D8), β-lactamase - *Acinetobacter baumannii* (UniProtKB: Q6DRA1), β-lactamase - *Klebsiella pneumoniae* (UniProtKB: Q9XB24), AmpC - Escherichia *coli* (UniProtKB: P00811), β-lactamase - *Aeromonas enteropelogenes* (UniProtKB: A0A175VLQ4 4).

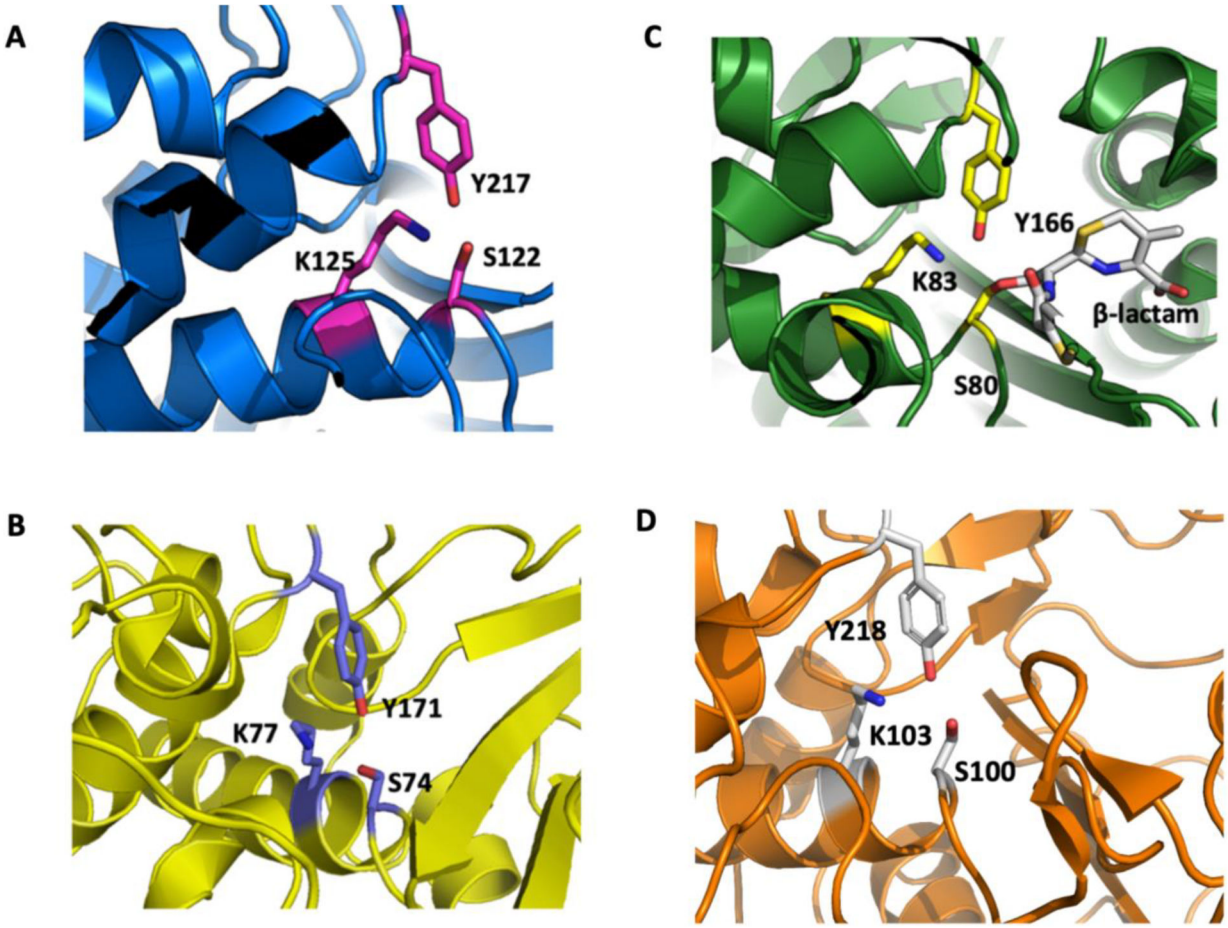

Figure 4.

Comparison of the active site of Lsa45. The catalytic triad (Ser, Lys and Tyr) responsible by catalysis is shown in sticks representation. The Ser amino acid is a nucleophile in α/β serine hydrolases. A) Lsa45 from *L. interrogans*, B) AD-peptidase from *B. cereus*, C) AmpC from *E. coli* and D) EstU1 from an uncultured bacterium.

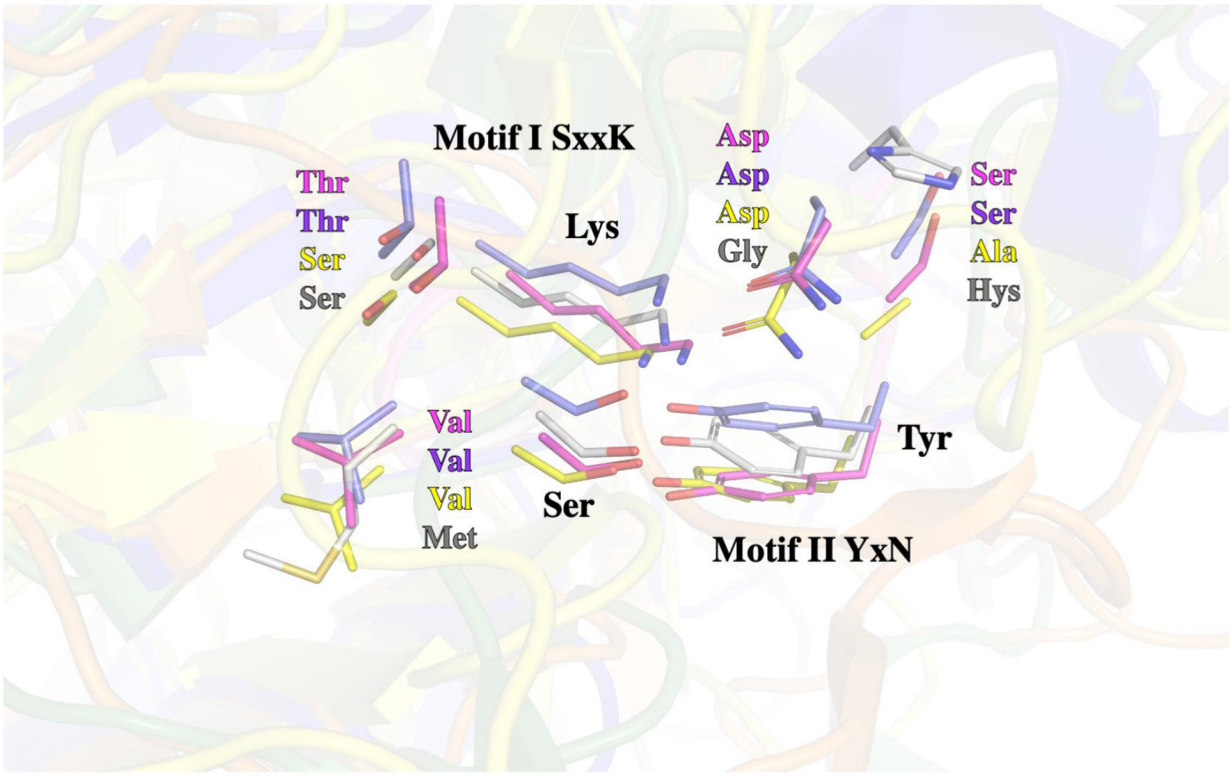

Figure 5.

Superposition of the catalytic residues of active Lsa45 with different enzymes. Serine and lysine residues belong to motif I (S*xx*K) and tyrosine residue comprises to motif II (Y*x*N). Lsa45 (magenta residues - PDB 8DC1), AD-peptidase (slate residues – PDB 4Y7P), AmpC (yellow residues – PDB 5GGW) and EstU1 (grey residues PDB 4IVK).

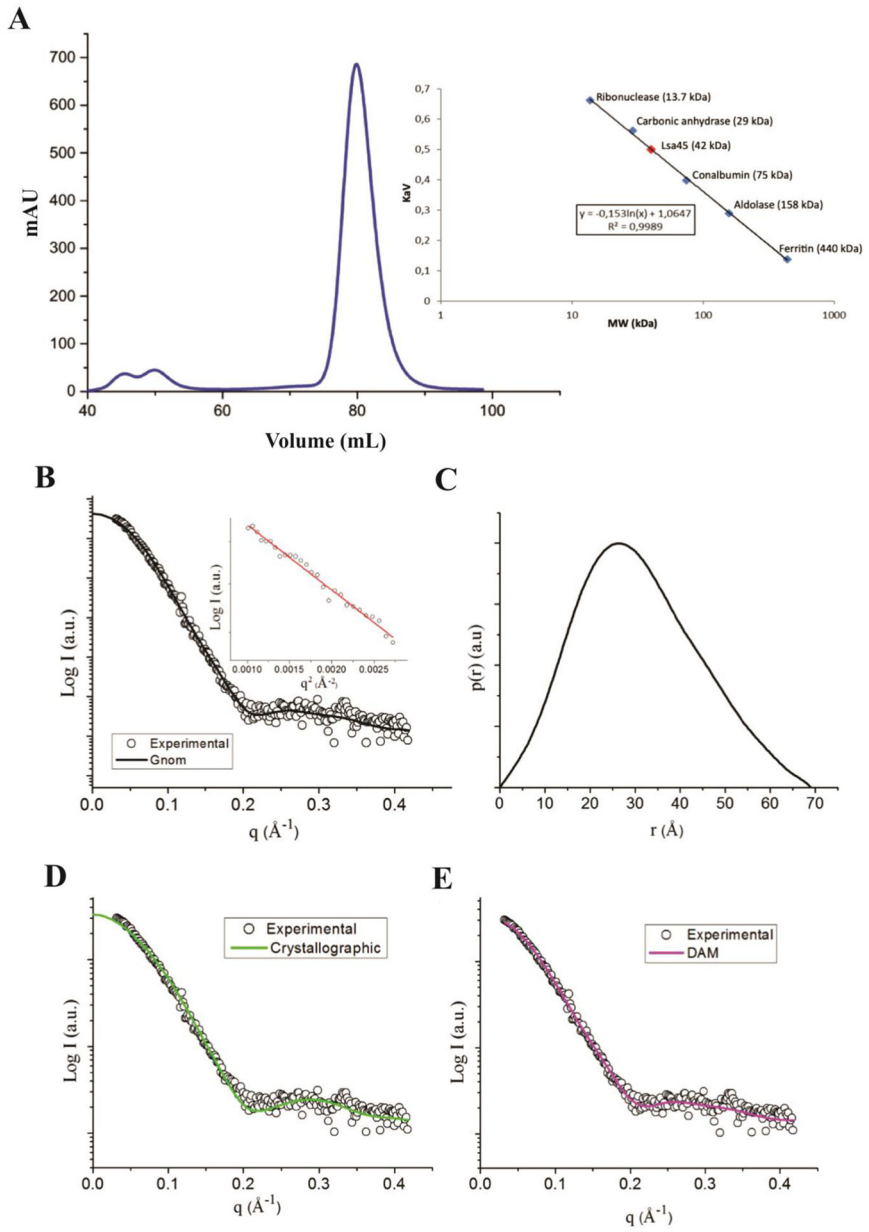

Figure 6.

Molecular mass analyses of Lsa45. A) The gel filtration chromatogram shows only one peak with a retention volume of 82.1 mL and an estimate of the molecular weight of Lsa45 plotted on the calibrated curve with molecular weights of known proteins suggests a value of 41 kDa. The predicted value after removing the signal peptide is 43 kDa. B) and C) Fitting of the experimental data and *p(r)* adjustment. C) Simulated scattering from the crystallographic structure and fit it to the experimental data. D) Dummy atoms model simulated scattering.

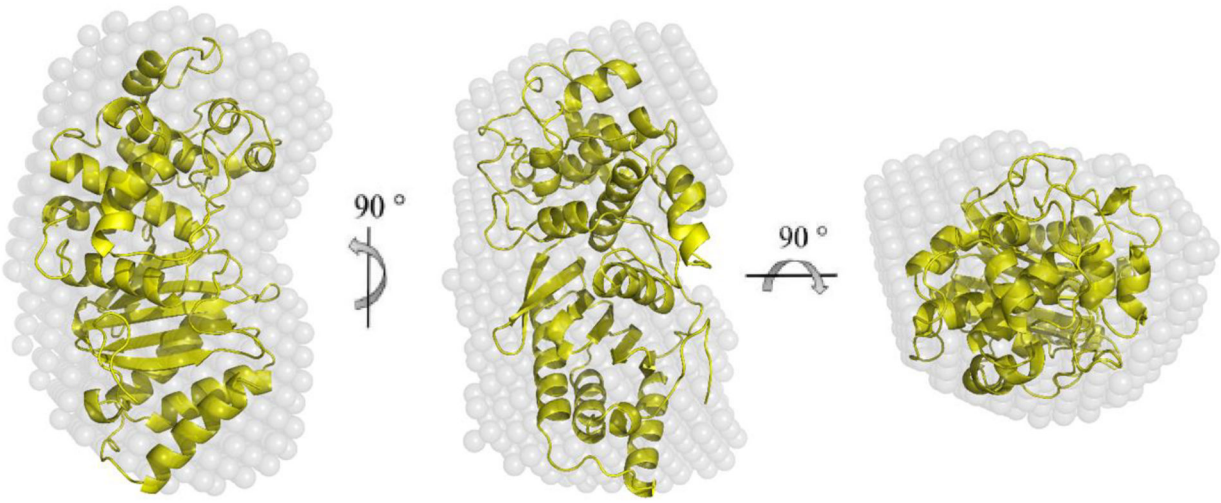

Figure 7.

Superposition of the crystallographic structure with the low-resolution dummy atoms model (DAM). The center and right models were rotated 90° around the y- axis and 90° around the x-axis from the orientation shown on the left panel.

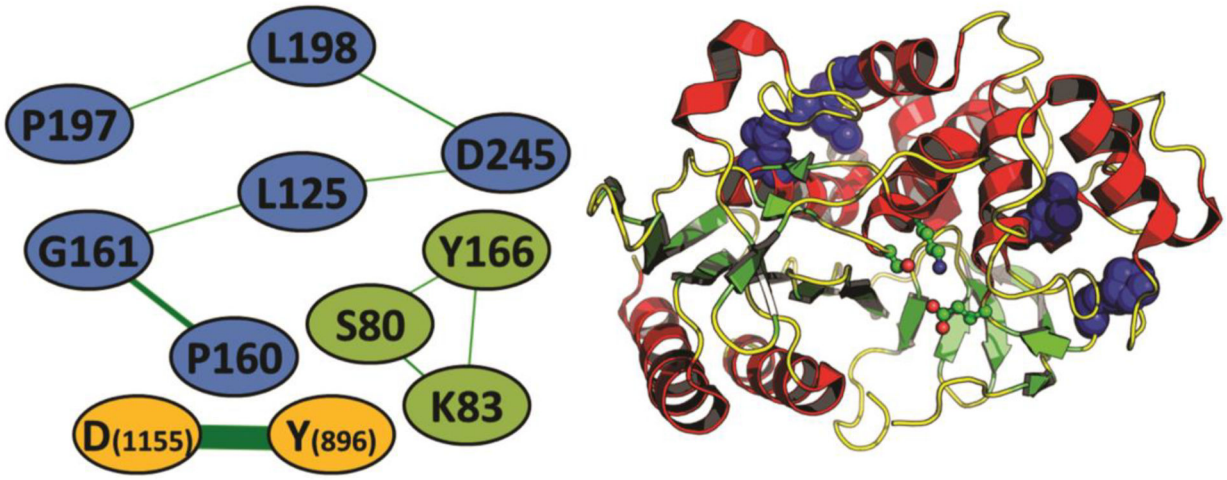

Figure 8.

Coevolution network analyses of Lsa45 A) The co-evolution network in the β-lactamase family. Nodes are connected whenever there is coevolution (e.g., the presence of a proline in position 160 is usually followed by the presence of a glycine in position 161 and vice-versa). Nodes are colored according to the three sets of coevolving residues found in the analysis. *E. coli* AMPC is used, except for of the D1155-Y896 coevolving pair, which uses the alignment numbering due to its absence in both AMPC or Lsa45. B) location of the six-residue coevolving set (blue spheres) in the three-dimensional structure of a β-lactamase (PDB code: 1FCM) when compared to the three catalytic residues (as balls-and-sticks).

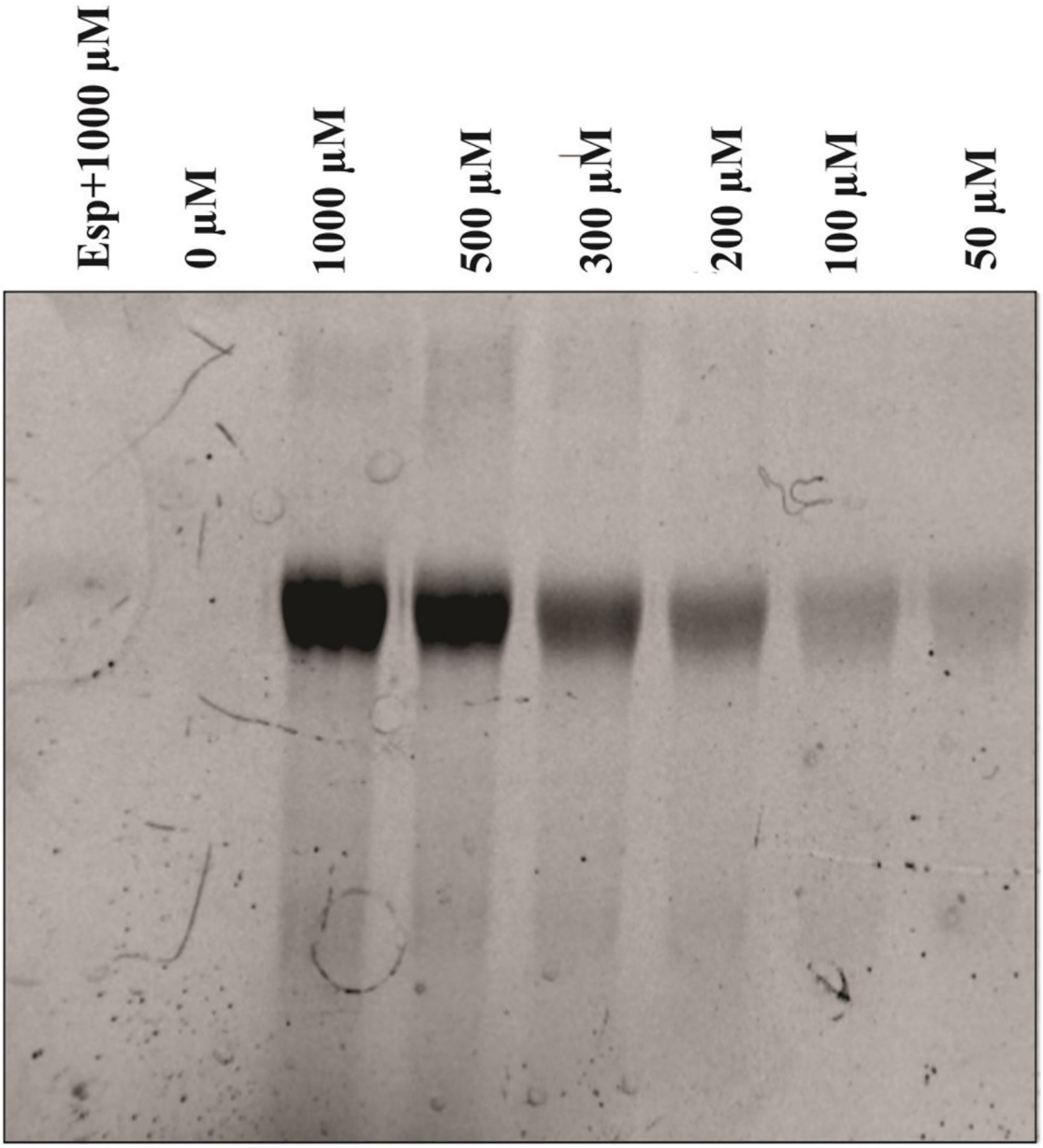

Figure 9.

Analysis of Bocillin FL binding with Lsa45. SDS-PAGE of the reaction mixture of Bocillin FL with Lsa45 was analyzed with different concentrations of Bocillin FL (0–1000 µM). A fragment of the enterococcal surface protein (Esp), which is a non-PBP, was used as a negative control.

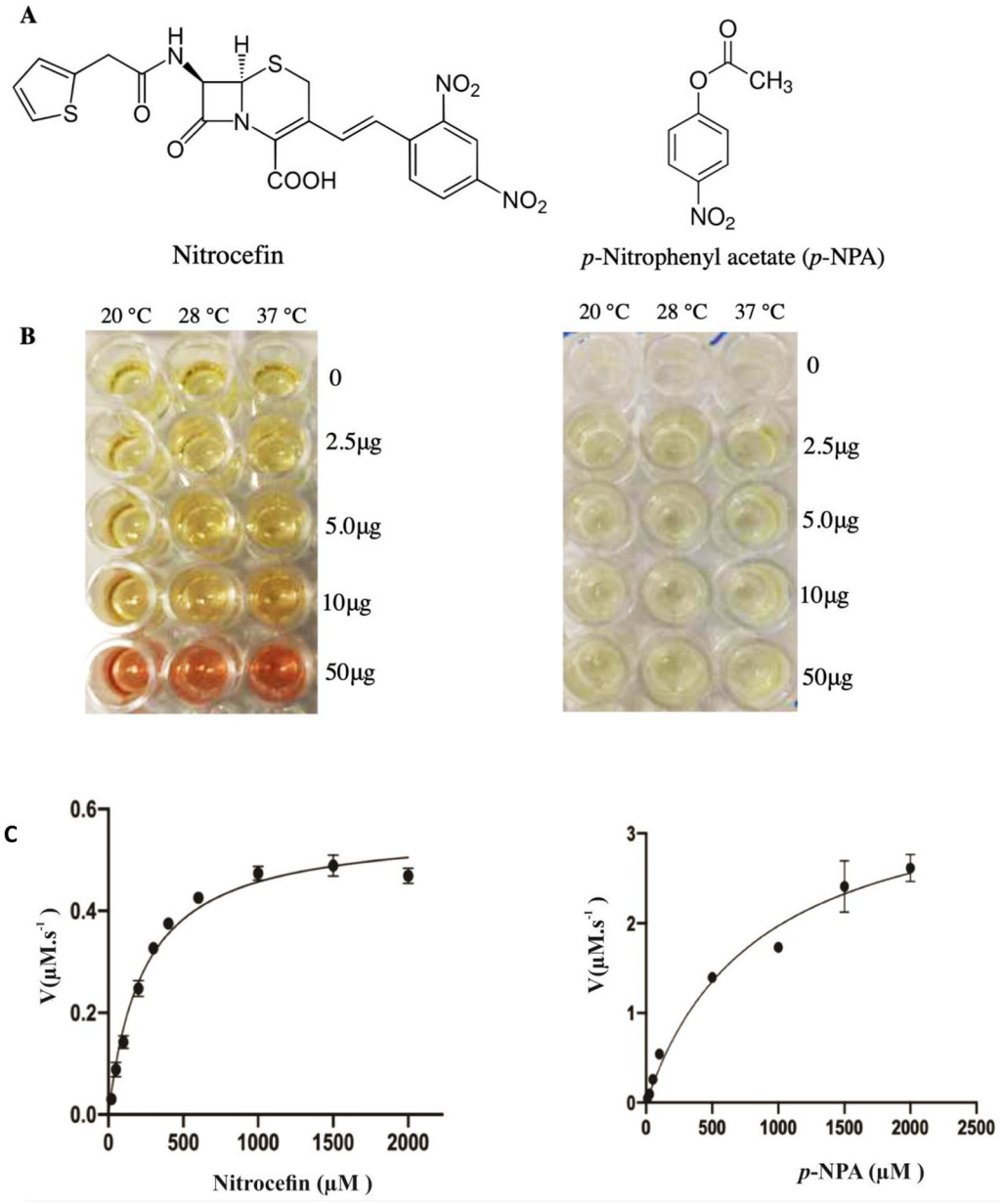

Figure 10.

Kinetic parameters for hydrolysis of nitrocefin and 4-Nitrophenyl acetate (*p*-NPA) by Lsa45. All measurements were completed in triplicate. Data were fitted to the Michaelis-Menten equation using Graphpad Prism8. A) Chemical structures of nitrocefin and *p*-NPA B) Kinetic activity of Lsa45 against nitrocefin C) Kinetic activity of Lsa45 against *p*-NPA.

Table 1.

Data collection and refinement statistics for Leptospiral surface adhesin of 45 kDa (Lsa45)[a]

Data Collection	
Beamline	LNLS – MX2
Wavelength	1.5499 Å
Resolution range (Å)	41.17–1.62
Space group	$P2_12_12_1$
Unit cell (a b c, Å)	44.14, 74.86, 113.47
Total reflections	1530015 (46424)
Unique reflections	48518 (4655)
Multiplicity	31.5 (20.9)
Completeness (%)	99.66 (96.95)
Mean I/sigma(I)	21.9 (2.1)
Wilson B-factor	17.11
$^{b}R_{pim}$	0.017 (0.619)
$CC_{1/2}$	0.999 (0.524)
Structure Refinement Statistics	
$R_{work}/^{c}R_{free}$	0.1978/ 0.2227
Protein atoms	2754
Ligand/ions	30
solvent	214
Protein residues	342
RMS (bonds) (Å)	0.010
RMS (angles)	1.35°
Ramachandran favored (%)	98.53
Ramachandran allowed (%)	1.18
Ramachandran outliers (%)	0.29
Rotamer outliers (%)	0.33
Clashscore	3.04
Average *B*-factor ($Å^2$)	23.0
Number of TLS groups	1
PDB ID	8DC1

[a]Statistics for the highest-resolution shell are shown in parentheses.

[b]$R_{pim} = \Sigma_h [1 / (n - 1)]^{1/2} \, h \, \Sigma_i | < I_h > - I_{h,i} | / \Sigma_h \, \Sigma_i \, I_{h,I}$, where h enumerates the unique reflections, i represents their symmetry-equivalent contributors, and n_h denotes multiplicity.

[c]R_{free} calculated with randomly selected reflections (5%).

Table 2.

Small-angle X-ray scattering (SAXS) structural parameters for Lsa45.

Parameters	Crystallographic	Experimental	Dummy Atoms Model
R_g (Guinier) (Å)	-	24.5	-
R_g (Å)	22.5	23.6	23.0
D_{max} (Å)	74.64	69.0	73.1
Mol. Weight (kDa)	44.7	46.3	-

Table 3.

Kinetic parameters of Lsa45 with nitrocefin and 4-Nitrophenyl acetate (*p*-NPA).

Substrate	K_m (μM)	Vmax (μM/s^{-1})	k_{cat} (s^{-1})	k_{cat}/K_m (μ$M^{-1}s^{-1}$)
Nitrocefin	235.0 ±6.40	0.5642 ±0.020	0.040 ±0.002	0.17
p-NPA	849.3 ±15.30	3.643 ±0.420	0.668 ±0.040	0.786